

Interfacial chemistry of Alq₃ and LiF with reactive metals

M. G. Mason,^{a)} C. W. Tang, L.-S. Hung, P. Raychaudhuri, J. Madathil,
and D. J. Giesen

Research Laboratories, Eastman Kodak Company, Rochester, New York 14650-2132

L. Yan, Q. T. Le, and Y. Gao

Department of Physics and Astronomy, University of Rochester, Rochester, New York 14627

S.-T. Lee, L. S. Liao, and L. F. Cheng

*Department of Physics and Materials Research, Center for Super Diamond Research,
City University of Hong Kong, Kowloon, Hong Kong, China*

W. R. Salaneck

Department of Physics (IFM), Linköping University, S-581 83 Linköping, Sweden

D. A. dos Santos

*Centre de Recherche en Electronique et Photonique Moléculaires, Université de Mons-Hainaut,
B-7000 Mons, Belgium*

J. L. Brédas

*Centre de Recherche en Electronique et Photonique Moléculaires, Université de Mons-Hainaut,
B-7000 Mons, Belgium and Department of Chemistry, The University of Arizona, Tucson,
Arizona 85721-0041*

(Received 14 April 2000; accepted for publication 18 September 2000)

The electronic structure and chemistry of interfaces between tris-(8-hydroxyquinoline) aluminum (Alq₃) and representative group IA and IIA metals, Al, and Al/LiF have been studied by x-ray and ultraviolet photoelectron spectroscopies. Quantum-chemical calculations at the density functional theory level predict that the Alq₃ radical anion is formed upon reaction with the alkali metals. In this case, up to three metal atoms can react with a given Alq₃ molecule to form the trivalent anion. The anion formation results in a splitting of the N 1s core level and formation of a new feature in the previously forbidden energy gap. Virtually identical spectra are observed in the Al/LiF/Alq₃ system, leading to the conclusion that the radical anion is also formed when all three of these constituents are present. This is supported by a simple thermodynamic model based on bulk heats of formation. In the absence of LiF or similar material, the reaction of Al with Alq₃ appears to be destructive, with the deposited Al reacting directly with the quinolate oxygen. We proposed that in those circumstances where the radical anion is formed, it and not the cathode metal are responsible for the electron injection properties. This is borne out by producing excellent injecting contacts when Ag and Au are used as the metallic component of the cathode structure. © 2001 American Institute of Physics. [DOI: 10.1063/1.1324681]

I. INTRODUCTION

A thin film, organic light emitting diode (OLED), such as indium-tin-oxide (ITO)/N,N'-bis-(1-naphthyl)-N,N'-diphenyl-1,1'-biphenyl-4,4'-diamine (NPB)/Alq₃/Mg:Ag, is a current injection device. The light output (electroluminescence) is derived from the radiative recombination of electrons and holes injected into the organic bilayer (NPB/Alq₃) from the respective metallic cathode (Mg:Ag) and the semi-transparent anode (ITO).¹ It has been well established that the electroluminescence efficiency (photons/charge) as well as the voltage required for the OLED is strongly dependent on the contacting electrodes and their charge injection characteristics.^{2,3} ITO glass, modified with an oxidative surface treatment, is commonly used as the hole-injecting contact,⁴⁻¹⁰ while a low work function metal (Mg, Ca, or Li)

or a metal alloy (Mg:Ag) is required to form an effective electron-injecting contact.^{1,2,11-13} These metals are poorly suited for a production environment because of their extremely high chemical reactivity. The ability to transition to Al cathodes would represent a significant advance in the practical development of OLED devices. Unfortunately, Al forms a rather poor cathode with high drive voltage and low efficiency for electron injection into Alq₃, the most common of electron transport materials. A significant step toward overcoming this problem was realized with the discovery that very small amounts of LiF or MgO at the Alq₃/Al interface drastically improved both the drive voltage and luminescence efficiencies.¹⁴ Likewise, doping of the near cathode portion of the Alq₃ with Li produced an excellent contact to Al.^{12,15} More recently a host of insulating materials has also shown similar beneficial effects. These include CsF,^{16,17} CsI,¹⁷ MgF₂,¹⁸ Li₂O, NaCl, KCl, K₂O, RbCl, and Cs₂O.¹⁹ Maximum efficiency enhancements are typically achieved at

^{a)} Author to whom correspondence should be addressed; electronic mail: max.g.mason@kodak.com

below-monolayer coverages and show a remarkable insensitivity to the exact compound employed. It has further been shown that the insulating materials need not be deposited as a film on the Alq₃ surface. At least in the cases of LiF^{16,20,21} and CsF,^{16,20} the insulators can be coevaporated with either the organic or metal at concentrations of about 3 at. % to give enhancements identical to those found in the thin film depositions. These similarities suggest similar mechanisms for electron injection in all cases. Because the formation of injection contacts is critical to the OLED device performance, numerous surface analytical studies have been undertaken, primarily using photoemission experiments, to characterize the injection barrier energetics and the chemical compositions at the anode/organic^{6–9} and cathode/organic^{3,22} interfaces. In our previous studies, we have examined in detail the ITO anode properties as a function of various oxidative treatments.⁸

In this study, we have focused our attention on the properties of the cathode/Alq interface where the cathode materials are low work function, group IA and IIA elements, Al, and LiF/Al. We use UPS and XPS combined with quantum chemical calculations to characterize the energetic levels and the chemical nature of the Alq/cathode interface. We will show that the low work function metals and either LiF/Al or CsF/Al, when deposited onto Alq₃, produce species which have virtually identical spectra in both the core and valence orbitals and differ significantly from those produced when Al is deposited onto Alq₃ in the absence of LiF. These observations, quantum chemical calculations, and consideration of bulk thermodynamic heats of formation lead us to propose that the Alq₃[−] radical anion is formed in the presence of either a low work function metal or LiF/Al or CsF/Al. Based on the similarities in device performance, this is probably true for all of the insulating materials referenced above when used in conjunction with Al.^{16–19}

II. EXPERIMENT

Measurements were made on three separate instruments. All spectra involving Li and K were recorded at Linköping University and these measurements have been previously described in detail.²³ Mg and Na measurements were performed at the City University of Hong Kong using a VG ESCALab 220i-XL spectrometer. All other measurements were made on VG ESCA Lab Mark II. Both of these latter instruments used monochromatic Al K_α radiation for all XPS spectra and unfiltered, He I radiation for UPS. Adjoining sample preparation chambers were present on both of these instruments and were used for vapor deposition of all samples. Base pressures were in the high 10^{−10} to low 10^{−9} mbar range in the preparation chamber. Pressures in the analysis chambers when the He lamp was not running ranged from 4 × 10^{−11} in the Mark II to about 2 × 10^{−10} in the ion pumped 220i-XL. Residual gas analysis of the 220i-XL analysis chamber showed He to be the primary ambient component. The typical instrumental resolution for XPS ranged from ≈0.4 eV to ≈0.8 eV, which yielded full width at half maximum values for the Ag 3d_{5/2} line of 0.79 and 1.2 eV. The poorer instrumental resolution was only employed to

increase the count rate of the extremely weak Li 1s level at low coverages where detection was extremely difficult. For UPS measurements the typical resolution ranged from ≈0.03 to 0.1 eV. For these measurements the samples were biased at −4.0 V to observe the true, low energy secondary cutoff and enhance the emission of the extremely low energy secondary electrons.

Alq₃, Ca, and Mg were thermally evaporated from Ta boats, LiF and CsF were evaporated from W filaments, and Al from a BN crucible. The nominal thickness for the Alq₃ was maintained at 100 Å. A SAES® alkali metal dispenser was used for the Na depositions. Optically flat Si(110) or (100) wafers were used for the evaporation substrates. Coverages were measured with a quartz crystal oscillator, which was calibrated by measurement of the XPS core level intensities or, in the cases of LiF, CsF and Alq₃, by the more accurate technique of spectroscopic ellipsometry.

III. RESULTS AND DISCUSSION

A. Low work function metals on Alq₃

The most accepted model for electron injection from a metal into an organic material such as Alq₃ requires that the metal have a relatively low work function.^{1,2} This is thought to be necessary so as to minimize the energy barrier between the metal Fermi level and the lowest unoccupied molecular orbital (LUMO) of the organic. The first systematic, photoemission study of such an interface involving Alq₃ was with alkaline earth metal Ca.^{24–26} At low coverages of Ca(Θ_{Ca} ≤ 4 Å), where the reaction with Alq₃ does not appear to be destructive, the photoemission spectra yield three significant clues as to the metal/organic interaction. In the XPS spectra the N 1s peak is split with a new feature appearing on the low binding energy (BE) side and having about one half the intensity of the stronger component. Also, the Ca core levels have unusually high binding energies characteristic of a divalent cation. Finally, in the UPS spectra, all of the Alq₃ molecular orbital features are shifted to higher binding energy and a new state is formed in the previously forbidden energy gap. This is shown in Fig. 1. These spectral modifications were taken as evidence for formation of the Alq₃[−] radical anion. This assignment was supported by semiempirical (ZINDO) molecular orbital calculation by Burrows *et al.*²⁷ that showed the excess electronic charge in the Alq₃[−] radical anion to be localized on the pyridyl side of one of the three quinolate rings. This highest occupied molecular orbital (HOMO) of the radical anion is closely identifiable with the LUMO orbital of the neutral molecule. More elaborate and accurate calculations have since been reported^{23,28} but the basic conclusions remain unaltered. This proposed electronic structure accounts for all of the spectral features highlighted above. The N 1s peak splits, with a 2:1 ratio because the charge density in the radical anion is localized on the pyridyl side of one of the quinolate rings. The ratio of 2:1 results from the charge being on only one of the three possible nitrogens. The high BE observed for Ca is due to the highly ionic character of the bonding with the Ca transferring two electrons to two different Alq₃ molecules. This is confirmed by XPS intensity measurements which show that, in

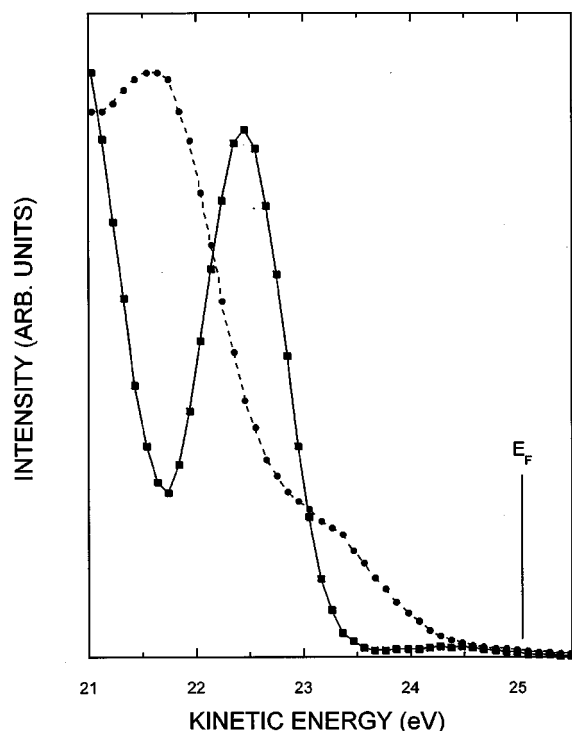


FIG. 1. The HOMO region of the UPS spectra for pristine Alq_3 (■) and Alq_3 after deposition of 0.5 Å of Ca (●).

this low coverage regime ($\Theta_{\text{Ca}} \leq 4 \text{ \AA}$), the amount of deposited Ca is approximately one half of the amount of N observed in the low binding feature in the $\text{N } 1s$ spectra. Finally, the gap state results from occupation of what was one of the triplet of empty LUMO orbitals in the neutral molecule.

This interpretation has been substantially strengthened by more recent work on Li,²³ K,²³ and Mg (Ref. 29) depositions on Alq_3 and our new results with Na and Mg. In Fig. 2(A), we show the low BE region of the UPS spectra for all five of the metals that we have studied. While there are some slight qualitative differences in intensity that result from variations in the metal coverage, the overall shape of the

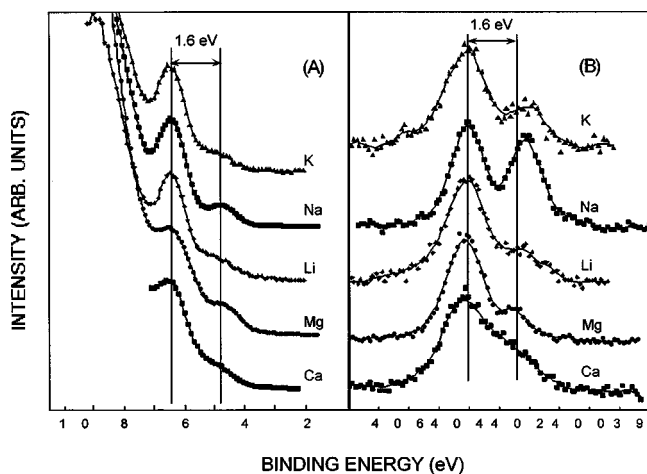


FIG. 2. The HOMO region of Alq_3 after deposition of group I and II metals (A) and the $\text{N } 1s$ region for the same series of metals (B). Binding energies are referenced to the vacuum level.

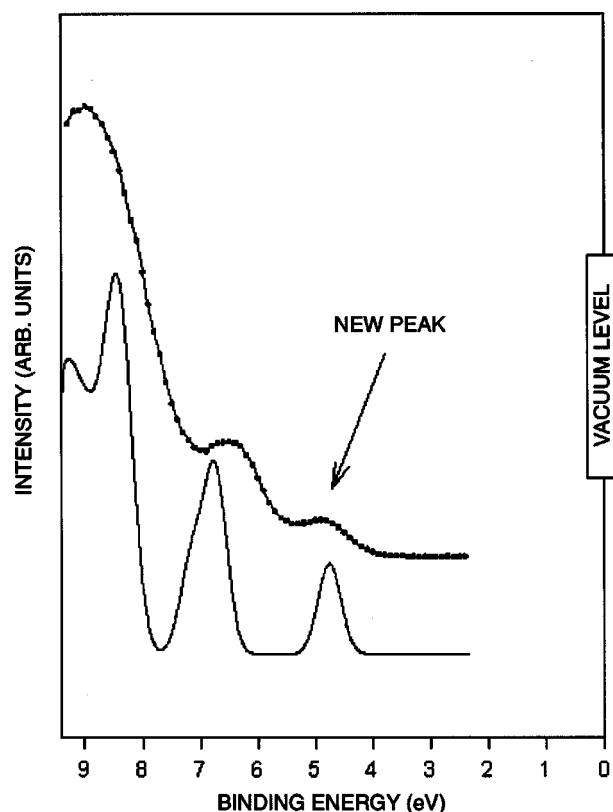


FIG. 3. Comparison between the experimental He I spectrum (upper curve) and the theoretical DOVS (lower curve), obtained from a generalized transition state calculation on the basis of the DFT formalism, corresponding to a doping level of one potassium atom per Alq_3 molecule. The calculated curve has been shifted to align with the experimental results.

spectra is remarkably similar. In all five cases, the original HOMO level is shifted to higher BE and the gap state is formed in the forbidden gap at an energy of $\approx 1.6 \text{ eV}$ above the shifted HOMO level. We have significantly extended the theoretical model from the earlier semiempirical calculations²⁷ to aid in the interpretation of these spectra. The theoretical UPS spectrum for the reaction product of K with Alq_3 was obtained by using the generalized transition state method³⁰ with the eigenenergies obtained from density functional theory (DFT) calculations as described in Ref. 23. Figure 3 shows a comparison of the top (lowest BE) portion of the valence region, where the experimental spectrum and theoretical density-of-valence-states (DOVS) are compared, both for a doping level corresponding to one potassium atom per Alq_3 molecule. The agreement between theory and experiment is excellent. The theoretical calculation predicts a slightly larger splitting ($\approx 1.9 \text{ eV}$), between the new state in the original forbidden energy gap and the peak corresponding to the old HOMO, than what is measured experimentally ($\approx 1.6 \text{ eV}$). The difference can, at least partly, be attributed to the fact that the calculation is performed in the ‘‘gas phase’’ with no polarizing medium surrounding the Alq_3 . Therefore, in the calculation, the extra electron that is added to the system is more strongly repelled by the other electrons in the molecule than in the real material where the repulsion is reduced by screening due to electrons on neighboring molecules. In agreement with our conclusions based on the ear-

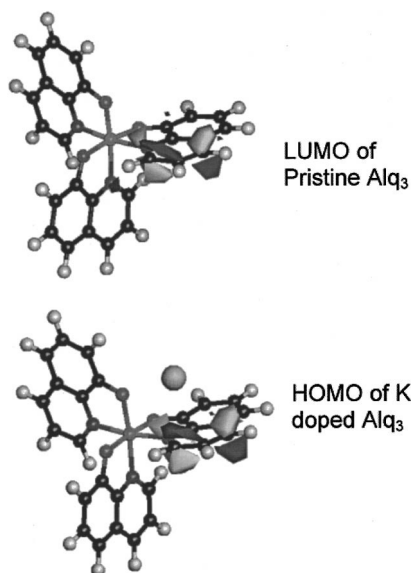


FIG. 4. Sketch of the pristine Alq₃ LUMO and the potassium doped HOMO as calculated at the gradient-corrected DFT level (Ref. 23).

lier calculations, these results also show that the new peak corresponds to the LUMO of pristine Alq₃, and that the previous HOMO has become HOMO-1. This is clearly seen in Fig. 4 where the new HOMO of potassium-doped Alq₃ is shown to be almost identical to the original LUMO of Alq₃. Further experimental evidence of this type of interaction is shown in Fig. 5 where a much larger portion of the UPS spectra of Alq₃ is shown for various coverages of Na. Evolution of the gap state discussed above is clearly observable on the high kinetic energy side of the spectra. The point to be made here is that the molecular orbital structure of Alq₃ appears to be preserved as the Na coverage increases. Identical behavior is observed for Li, K, and Mg deposition onto Alq₃.^{23,29} In fact, if these spectra are plotted with respect to the vacuum level rather than the Fermi level, their positions are independent of metal coverage. The spectral region covered by these scans encompasses all of the π and much of the σ bonding regions of Alq₃.³¹ The fact that emission from these states is, aside from some broadening, independent of metal deposition, strongly suggests that the basic Alq₃ structure is preserved. The reaction product of these metals with Alq₃ must not involve any significant modification of the Alq₃ structure such as bond breaking or rearrangement.

The other spectral feature that we have identified as a characteristic of the formation of the Alq₃⁻ radical anion is the splitting of the N 1s spectra. This region is shown in Fig. 2(B) for this same set of five metal overlayers on Alq₃. Two features appear to be somewhat at odds with the interpretation presented above: the splittings appear to be metal dependent and the intensity ratios can, quite clearly, differ from 2:1. The metal dependence of the splitting is simply related to the ionicity of the “bond” between the metal and Alq₃. The lower the ionization potential, the more easily the electron can be removed from the metal and the more ionic the “bond” will be. Therefore, the unique nitrogen will have a greater charge when the bond is more ionic and this will be reflected in a larger spectral shift. The ionization potential is

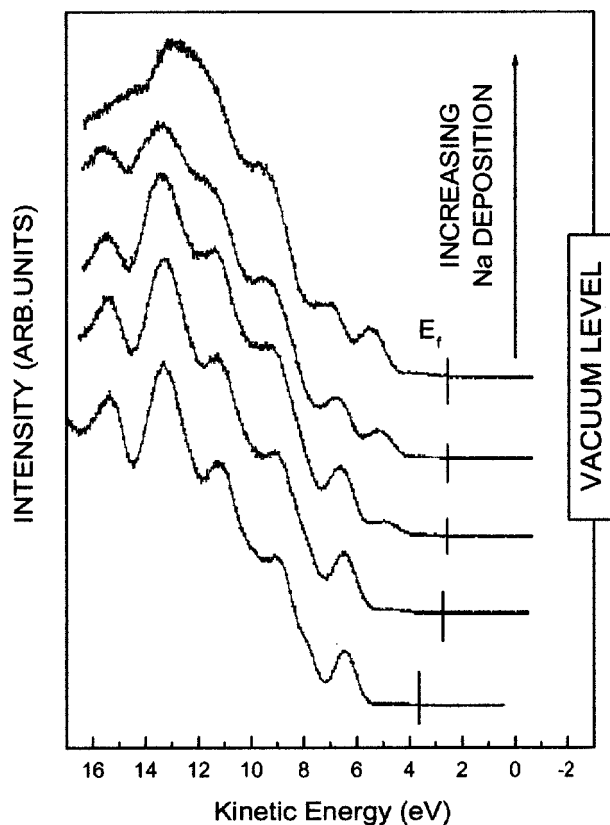


FIG. 5. Evolution of the valence band spectrum with increasing Na doping. Note the appearance of the gap state on the high kinetic energy side of the HOMO and continued presence of the molecular orbital structure even at the highest level of metal doping.

a measure of the ease of removing an electron and increases in the order $K < Na < Li < Ca < Mg$. Within experimental uncertainty, this correlates well with the order of decreasing splitting. The metal dependence of the peak intensity ratios points out an apparent, significant difference between the alkali metals (Li, Na, and K) and alkali earth metals (Ca and Mg). Given a sufficient supply of metal atoms, the group IA, alkali metals are able to donate up to three electrons to Alq₃ to form the Alq₃⁻³ radical anion.²³ At the level of three metal atoms per Alq₃, each of the three different ligands has received one extra electron charge, resulting in just one corresponding peak in the N 1s spectrum.²³ This effect is illustrated in Fig. 2(B). The Li and K coverages in this figure are close to one alkali atom per Alq₃ molecule but the Na coverage is considerably higher and is reflected in an increased intensity in the low binding energy component. If the alkali metal concentration is increased further, the low binding energy component will continue to increase in intensity to the point where it is the sole peak. As discussed in detail in Ref. 23, this is the signature for formation of the trivalent Alq₃⁻³ radical anion. In the case of the group IIA, alkali earth metals Ca and Mg, this does not happen. Both of these metals appear to donate only one electron to each of the two Alq₃ molecules, regardless of the amount of deposited metal. In the case of Ca, it is believed that the metal diffuses in only to a depth of ≈ 10 – 12 Å.³² If the metal deposition is increased above a critical coverage of ≈ 4 Å, a destructive reaction occurs in which the metal appears to attack at the phenoxy

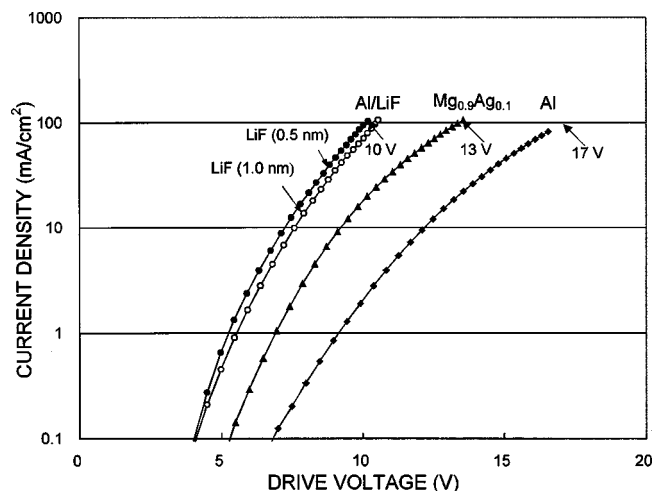


FIG. 6. Current–voltage characteristics of four EL devices using an Al, a $Mg_{0.9}Ag_{0.1}$, and an Al/LiF electrode, respectively.

oxygen^{24,26,32} and destroy the Alq_3 molecular structure. Mg, perhaps because of its smaller size and lower reactivity, behaves quite differently. Like Ca, it produces only the singly charged radical anion of Alq_3 , but shows no evidence of destructive reaction regardless of the amount of metal deposited and appears to diffuse more deeply into the Alq_3 substrate.²⁹

B. Aluminum on Alq_3

$Ca^{2,11,33}$ and $Mg^{1,2,11,13,34}$ are both known to make excellent electron injecting contacts. The alkali metals themselves are too reactive for use in device fabrication but doping of Al with Li has been shown to also produce very good electron injecting contacts.^{12,35} From the standpoint of commercial device fabrication, there would be significant advantage in completely eliminating these reactive, group IA and IIA metals. In this sense, a pure Al cathode would be very desirable. Unfortunately, as shown in Fig. 6, Al makes a fairly poor cathode in Alq_3 based devices when compared to $Mg_{0.9}Ag_{0.1}$. This may seem surprising in that studies of Alq_3 deposited on Al show a very small barrier to electron injection.^{22,36,37} In an effort to understand the relatively poor electron injection in Al/ Alq_3 based devices, we have studied the interface formation produced from Al deposition onto Alq_3 .³⁸ This is the deposition sequence actually used in conventional device fabrication and is the reverse of that in Refs. 22, 36, and 37. In Fig. 7(A) we show the evolution of the Al $2p$ spectrum as Al metal is deposited onto Alq_3 . The bottom curve is from pristine Alq_3 and shows a peak with a binding energy characteristic of Al in an oxidized state, the condition to be expected in Alq_3 . With increasing coverage of deposited Al, this peak grows in intensity and broadens fairly symmetrically until a coverage of $\Theta_{Al} \approx 4 \text{ \AA}$, where a new, low binding energy feature is distinctly observable. This peak continues to grow with increasing Al deposition and evolves into a peak characteristic of the metallic state. Both the N $1s$ and O $1s$ spectra significantly broaden and develop shoulders to the low and high binding energy sides, respectively. The C $1s$ simply broadens symmetrically with increasing Al

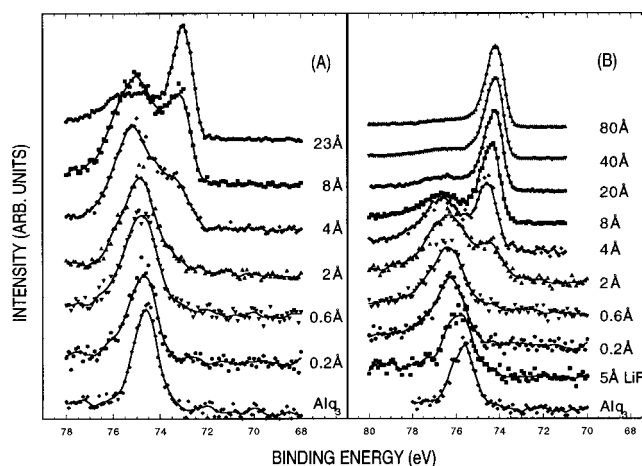


FIG. 7. Evolution of the Al $2p$ spectrum with increasing Al deposition on pristine Alq_3 (A) and Alq_3 with 5 \AA of LiF (B).

deposition. The simplest interpretation of these spectra is that in the first 2–4 \AA of deposited Al, the metal destructively reacts with the Alq_3 molecule. This is supported by the UPS spectra in Fig. 8. These spectra stand in marked contrast to those in Figs. 2(A) and 5, where the Alq_3 molecular orbital structure is well preserved with metal deposition. In the present case, as little as 0.2 \AA of Al is sufficient to almost destroy the well-defined spectral structure. Both the XPS and UPS are consistent with a destructive reaction between Al and Alq_3 that is limited to slightly less than 4 \AA of deposited metal. Above this coverage the metallic peak appears in the XPS spectrum and a weak Fermi level is observable in the UPS.

While the electron spectroscopy is very indicative of a significant chemical reaction it provides little information as

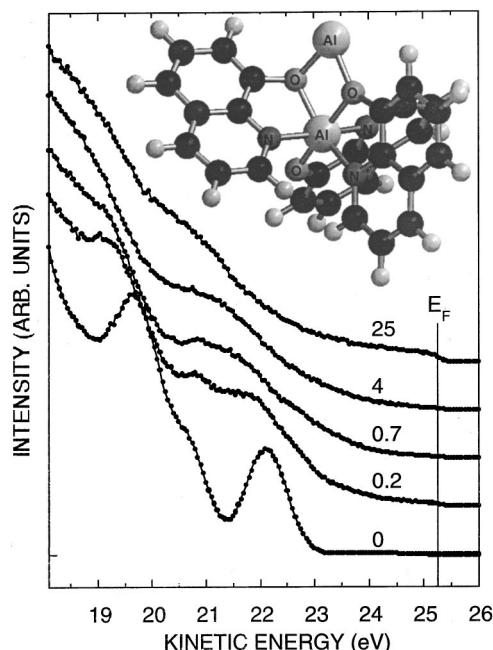


FIG. 8. Evolution of the valence band spectrum of Alq_3 with increasing Al deposition. The inset shows the molecular structure of the reaction product between an Al atom and an Alq_3 molecule as predicted by DFT calculations.

to the chemical structure of the reaction product. To further our qualitative understanding of the possible chemistry at this interface, we have performed quantum chemical calculations using the DFT for the interaction of a single Al atom with an isolated Alq₃ molecule.³⁹ These calculations predict that the incoming Al will bond directly to oxygen atoms on two of the three quinolate rings as shown in the insert in Fig. 8 and is very similar to the structure recently published by Curioni and Andreoni.⁴⁰ The actual reaction product in the solid state, where there is an excess of Alq₃, may be quite different as Al is seldom found in a two coordinated state. However, the observed spectral changes are consistent with these results and supportive of a strong Al–O interaction. The relatively poor performance of Al for electron injection into Alq₃ is probably due to the formation of this reacted layer in the device fabrication. Because of the large size of the Alq₃ molecule, 2–4 Å of deposited Al could produce a reacted layer of more than 100 Å and significantly modify the charge injection properties of the interface.

C. Aluminum on LiF on Alq₃

We have previously shown that when a small amount of LiF or MgO is present at the Al/Alq₃ interface, the device performance is significantly improved.¹⁴ The drive voltage, Fig. 6, is lowered and the electroluminescence efficiency enhanced. Since that discovery, several other materials have been found to produce similar results.^{16–19} Also, it has further been shown that LiF and CsF can be coevaporated with either the Al cathode material^{16,21} or the Alq₃ electron transport material^{20,21} to produce similarly enhanced charge injection. The improvements in charge injection have been largely ascribed to one of three possible effects. The barrier between the cathode Fermi level and the organic HOMO may be lowered by either decreasing the metal work function^{41–44} or creating a voltage drop across a layer formed by the insulating material.^{14,18,45–47} Alternatively, interfacial gap states in the organic film may be eliminated.⁴⁸ The fact that as little as the weight equivalent of 1 Å of LiF can cause a very substantial improvement in charge injection argues against those models requiring the presence of an actual insulating layer. Likewise, the enhanced performance of devices constructed with LiF:Al^{16,21} or CsF:Al (Ref. 16) composite cathodes or LiF:Alq₃^{20,21} or CsF:Alq₃ (Ref. 20) mixed transport layers is inconsistent with the insulator layer model.

Our first goal in characterizing the Al/LiF/Alq₃ interface was to try to determine if the evaporated LiF undergoes any reaction in the process of interface formation. We studied LiF evaporated onto Al and onto Alq₃ as well as Al onto LiF. Stoichiometry was determined from the integrated areas of the F and Li 1s peaks after correction for ionization cross sections and instrumental transmission function. The accuracy of these measurements is limited by the extremely low ionization cross section of the Li 1s emission.⁴⁹ However, in all three experimental variations the Li:F ratio was, within experimental error, identical to that of thick films prepared on a gold substrate. The chemical state was monitored by the splitting between the F and Li 1s peaks and by the F Auger parameter.⁵⁰ Again, within experimental error, these values

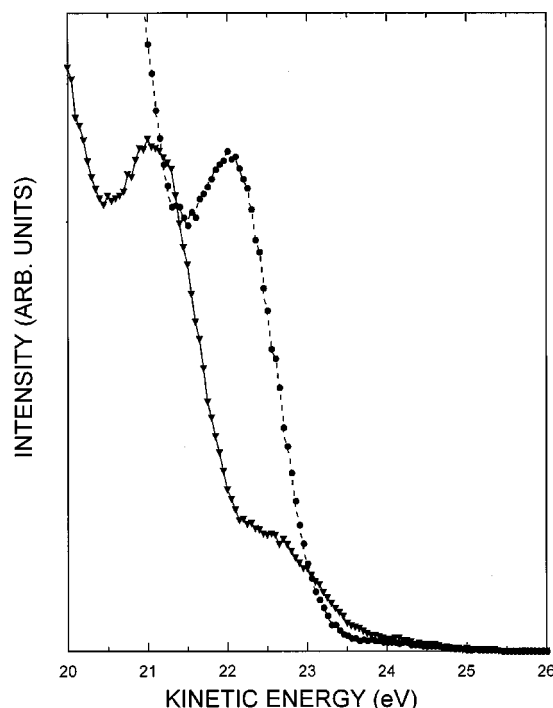


FIG. 9. The HOMO region of the UPS spectra of Alq₃ with 5 Å of LiF (■) and the same sample after deposition of 0.2 Å of Al (▼).

agreed with those of bulk LiF. In these model experiments, there is absolutely no evidence that the LiF has undergone any significant chemical modification. We concluded that to understand the charge injection process it is necessary to study the actual ternary interface!

In Fig. 7(B) we show the evolution of the Al 2p line with increasing Al deposition. The bottom-most spectrum is for pristine Alq₃ and the one above it is with 5 Å of LiF deposited onto the Alq₃. This series of spectra is similar to those in Fig. 7(A) in that the peaks broaden and shift to higher BE with increasing metal deposition and above a certain coverage, a peak which is characteristic of the metallic state begins to appear. Two major differences are apparent. The BE shifts in the presence of LiF are considerably larger regardless of whether the reference is taken with respect to the Fermi or vacuum level. Also, when the LiF is present, the metallic-like peak is observed at a considerably lower coverage of deposited Al. Based on the appearance of the metallic peak at a lower Al coverage, we conclude that one of the effects of LiF is to “protect” the Alq₃ from the deleterious reaction with Al. However, we do not believe this to be the most significant effect. In Fig. 9 we show the HOMO region of Alq₃ with a 5 Å deposition of LiF and the same spectral region after the deposition of only ≈0.2 Å of Al. The effect here is virtually identical to that observed when the low work function metals are deposited directly onto pristine Alq₃. This is illustrated further in Fig. 10(A) where spectra with both Al/LiF and Al/CsF overlayers are compared to those with pure metal overlayers. In the case of the simple metallic depositions, the spectral changes in this region were ascribed to the formation of the Alq₃⁻ radical anion. Formation of this species was also associated with a splitting of the N N 1s signal as a result of the localization of

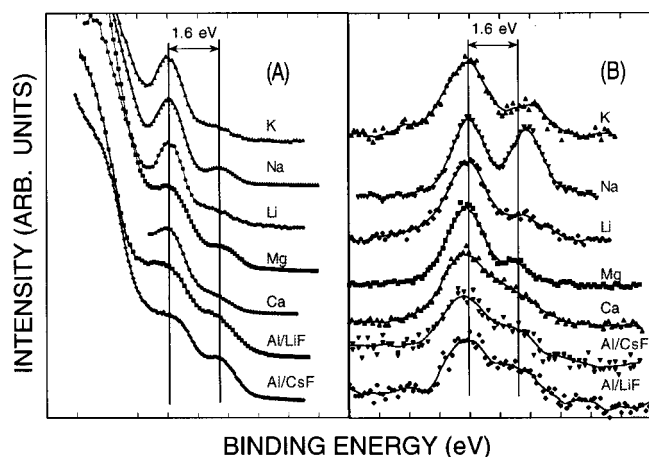
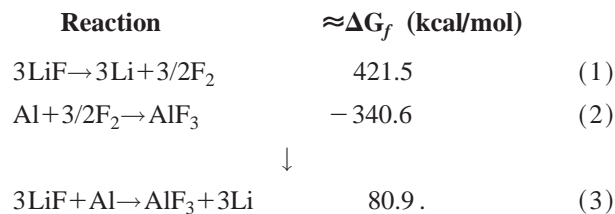


FIG. 10. The HOMO region of Alq_3 after deposition of Al/CsF, Al/LiF, group I metals, and group II metals (A) and the N $1s$ region for the same series of samples (B). The Al/LiF and Al/CsF spectra have been arbitrarily aligned with those of the pure metals (Ref. 51).

charge in the radical anion. In Fig. 10(B) we compare the N $1s$ spectra for the Al/LiF and Al/CsF overlayers with those of the simple metals. The agreement is excellent, especially considering the fact that the spectra were recorded in three different laboratories using spectrometers of different designs.

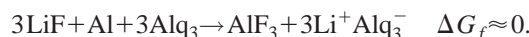
To understand these results, we propose that, in the presence of Alq_3 and Al, LiF and many other group IA and IIA metal halides or oxides react to produce the Alq_3^- radical anion. This species is responsible for both the gap state and the splitting of the N $1s$ peak. This may seem unlikely in view of the extremely small amount of Al that is required and also the exceptional chemical stability of LiF. The objection is accounted for by the large difference in size between an Al atom and an Alq_3 molecule. Consideration of this size disparity shows that $\approx 0.2 \text{ \AA}$ of Al corresponds to approximately one Al atom for each surface Alq_3 molecule. Therefore, a small volume of metal can react with a much larger volume of the organic material.

The issue of the stability of LiF is addressed by considering both calculated and known bulk heats of formation. The Gibbs free energy of formation ΔG_f for bulk LiF is 140.5 kcal/mole.⁵² Even the single bond dissociation energy is a very high 138 kcal/mole.⁵³ As shown below, the primary reason that LiF decomposes in this environment is due to the highly exothermic reaction of F with Al



Equation (3) shows that the free energy required to form Li has decreased from 140.5 to ≈ 26.9 kcal/mol, simply because of the exothermic nature of the AlF_3 formation. The overall reaction is still considerably endothermic and consistent with our experimental findings that no reaction occurs when LiF is evaporated on Al or Al onto LiF. The heat of reaction

between Li and Alq_3 to form the radical anion is not known experimentally. However we have calculated, using the DFT formalism, ΔH for the gas phase reaction between K and Alq_3 and it is exothermic by about -27 kcal/mol. These calculations show this to be a very ionic species, which means that ΔG_f should not be terribly sensitive to the metal cation as long as its ionization potential does not differ too much from that of K. This leads to the conclusion that for the overall reaction



Several points should be emphasized regarding this model. First the use of bulk thermodynamic data is a severe approximation. The LiF exists as a very thin film or, more likely, as isolated small clusters or molecules and the Al arrives at the surface as thermally hot atoms. These species are expected to have much greater chemical reactivity than their bulk counterparts. Also, while there is some indication in the Al $2p$ spectra that AlF_3 may be present, we have no experimental evidence for the existence of Li^+ . The weak intensity of Li emission and the BE shifts expected for small metallic clusters⁵⁴ makes it virtually impossible to determine the chemical state of Li. This model is more of a feasibility statement that shows that when LiF, Al, and Alq_3 are all present, the formation of the Alq_3^- radical anion is entirely reasonable. We have chosen one chemically simple pathway to illustrate the point.

D. Implication for device structure

Historically, the problem of electron injection at the cathode has been treated in terms of the orbital energies of the metal and the electron transporting material. This may still be the case in the Al/LiF/ Alq_3 type structures. It is possible that the enhanced injection is due to a reaction between the liberated Li and the Al metal to form a lower work function cathode^{13,35} and that the Alq_3^- radical anion is simply a passive byproduct. Alternatively, the reacted layer which is formed in the Al/LiF/ Alq_3 system may, itself, control the electron injection process. If this is true, then the injection is determined by this layer and not by the metal cathode material. This is essentially the model proposed by Kido and Matsumoto⁵⁵ in their work with layers of Li doped Alq_3 between the metal cathode and electron transport layer. If this model is indeed correct, then even high work function metals such as Au should form a good cathode when used in conjunction with Al/LiF. In Fig. 11 we show the luminance output of two test cells constructed with 250 \AA thick Au cathodes. The only difference was that one of the cells had 3 \AA of LiF and 10 \AA of Al deposited onto the Alq_3 prior to the Au deposition. The presence of the Al/LiF layer increased the light output by more than a factor of 100. Likewise Ag which is, at best, a poor cathode material works very well when the Al/LiF layer is present.

The ability to choose cathode materials without regard for their work functions gives considerably greater latitude in device design. Of particular interest is the development of surface-emitting devices where the entire cell is constructed on silicon and the light is emitted through a transparent top

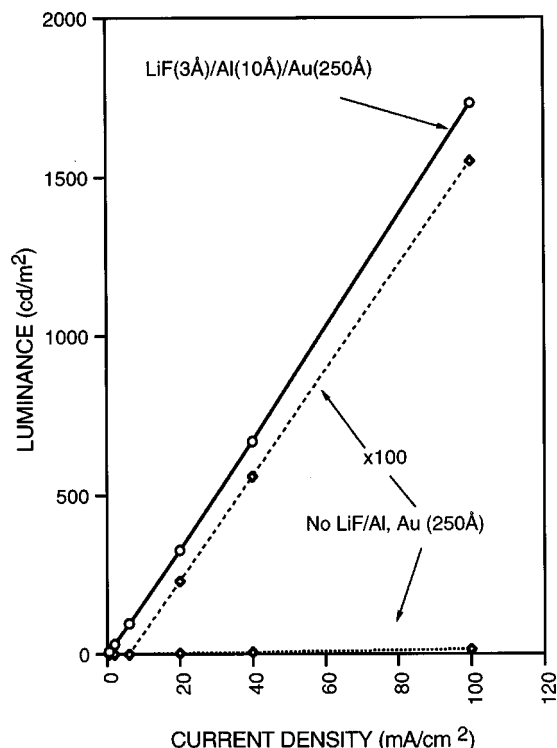


FIG. 11. Luminance output-current density characteristics of a cell with the configuration ITO/NPB/Alq₃/Au and for an ITO/NPB/Alq₃/LiF(3 Å)/Al(10 Å)/Au configuration.

electrode.⁵⁶⁻⁵⁹ Several schemes have been developed to extract light through the cathode^{56,58} but only recently has a process evolved having reasonably good surface emission characteristics.⁵⁹ This was achieved using a multilayer structure of ITO glass/copper phthalocyanine (CuPc)/NPB/Alq₃/CUPC/Li followed by sputter deposition of ITO. XPS analysis established that Li diffused through the CuPc and was available to dope the Alq₃. Li doping of such an interface involving Alq₃ would most likely produce the Alq₃⁻ radical anion and give the type of enhanced performance we have demonstrated. To investigate the utility of the Al/LiF/Alq₃ structure as part of a surface-emitting device, a multilayer structure was employed with a configuration of ITO/NPB/Alq₃/LiF(3 Å)/Al(6 Å)/Ag(200 Å)/R. R was either Alq₃ or MgO and is used for refractive index matching to optimize optical transmission. The luminance and current-voltage characteristics of one such device (R=Alq₃) is shown in Fig. 12. The insensitivity of the injection to the specific metal allows us to use Ag, which has far superior optical properties to Mg₉₀Ag₁₀ and 2 orders of magnitude better conductivity than ITO. This device has a luminance output of more than 500 cd/m² from the cathode side at a current density of 20 mA/cm².

IV. CONCLUSIONS

We have shown that when low work function metals are deposited onto Alq₃ a charge-transfer type of reaction occurs in which the Alq₃⁻ radical anion is formed. In the case of the group IA alkali metals, up to three electrons can be transferred to form the Alq₃³⁻ anion with each excess electron

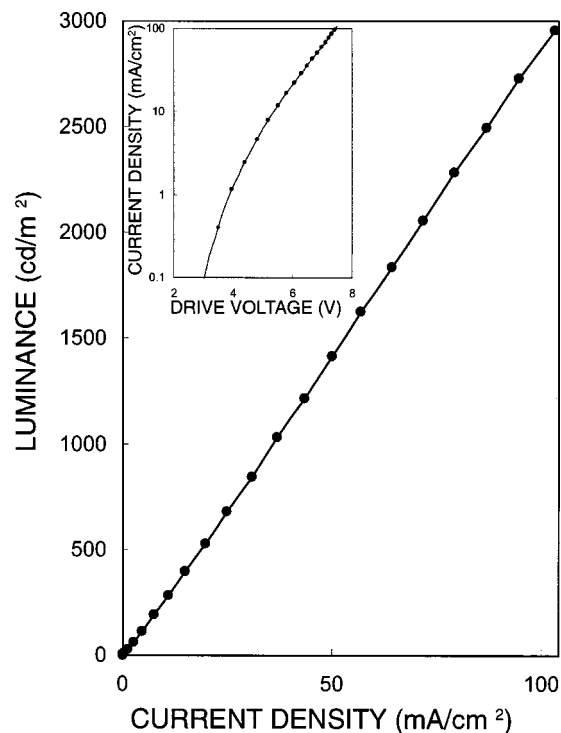


FIG. 12. Luminance-current and current-voltage characteristics for a cell with the configuration ITO/NPB/Alq₃/LiF(3 Å)/Al(10 Å)/Ag(200 Å)/Alq₃.

coming from a distinct alkali atom. When the reaction is with the group IIA, alkali-earth metals Ca or Mg, it is limited to formation of the singly charged radical anion with each metal atom donating an electron to two different Alq₃ molecules. In each case the charge is localized on the pyridyl side of the quinolate ligand. In the multiply charged anions, which are formed at higher doping levels of the alkali metals, the subsequent electrons are not transferred to the same ligand. There is never more than one excess electron per ligand because of the large Coulomb repulsion energy associated with putting a second electron onto such a relatively small ligand.²³ The excess charges occupy states that constitute the HOMO of radical anion and look very much like the LUMO of the neutral molecule. In the photoemission, these states are characterized by core and valence level shifts to higher binding energy and a splitting if the N 1s emission, and are directly observed as a new state in what was the forbidden energy gap of the neutral molecule.

When Al is deposited on to Alq₃ a destructive reaction appears to take place. All photoemission peaks, including the UPS, valence spectra, are significantly broadened or split. The observed spectra are consistent with the Al-Alq₃ reaction product predicted by DFT calculations. This reaction is limited to a thin surface layer and appears to be complete at $\Theta_{\text{Al}} < 4 \text{ \AA}$. It should also be noted that this type of reaction does not occur when Alq₃ is deposited onto bulk Al. This again emphasizes the point that the order of interface deposition is extremely important in determining the interfacial chemistry and studies in which the interfaces are not formed in the proper sequence may not reveal anything relevant to device performance. Based on the results of Alq₃ on Al,^{22,36,37} one might expect this to be an excellent injecting

contact but it is not! When the interface is made in the order actually used in device fabrication, this destructive reaction is observed and the relatively poor performance is understandable.

When an extremely small amount of LiF, or many other oxides or halides of the group IA and IIA metals is present during Al deposition onto Alq₃, a much improved contact is created. The LiF serves to somewhat reduce the extent of the reaction with Al. Metallic Al is observed at $\Theta_{\text{Al}} < 2 \text{ \AA}$, about half the coverage required in the absence of LiF. We believe that a more significant effect is the formation of a layer containing the Alq₃⁻ radical anion. Spectra observed with either Al/LiF/Alq₃ or Al/CsF/Alq₃ are virtually indistinguishable from those with the simple group IA or IIA metal overlayers. While the mechanism for charge injection from this layer is not yet understood, it does appear that this layer controls the injection process and that the metallic component of the cathode is relatively unimportant. This realization allows for much greater flexibility in design of cathode structures. We have made highly efficient cells using both Ag and Au as the cathode metal and have applied this type of structure to create promising surface emitters as will be required for silicon-based, active matrix displays.

ACKNOWLEDGMENTS

This work was supported, in part, by DARPA Grant No. DAAL01-96-K-0086 and NSF Grant No. DMR-9612370. The Mons-Linköping collaboration is supported by the European Commission within a Training and Mobility of Researchers (TMR) Network (SELOA, Project No. 1354) and within a Brite/EuRam project (OSCA, Project No. 4438). The work in Mons is partly supported by the Belgian Federal Government "InterUniversity Attraction Pole on Supramolecular Chemistry and Catalysis (PAI 4/11)," and FNRS-FRFC. Research on condensed molecular solids and polymers in Linköping is supported in general by grants from the Swedish Natural Science Research Council (NFR), the Swedish Research Council for Engineering Sciences (TFR), and the Carl Tryggers Foundation. The authors would also like to acknowledge many useful discussion with Ralph H. Young.

¹C. W. Tang and S. A. VanSlyke, *Appl. Phys. Lett.* **51**, 913 (1987).

²I. D. Parker, *J. Appl. Phys.* **75**, 1656 (1994).

³W. R. Salaneck, S. Stafström, and J. L. Brédas, *Conjugated Polymer Surfaces and Interfaces* (Cambridge University Press, Cambridge, 1996).

⁴C. C. Wu, C. I. Wu, J. C. Sturm, and A. Kahn, *Appl. Phys. Lett.* **70**, 1348 (1997).

⁵F. Li, H. Tang, J. Shinar, O. Resto, and S. Z. Weisz, *Appl. Phys. Lett.* **70**, 2741 (1997).

⁶T. Osada, Th. Kugler, P. Bröma, and W. R. Salaneck, *Synth. Met.* **96**, 77 (1998).

⁷F. Nüesch, L. J. Rothberg, E. W. Forsythe, Q. T. Le, and Y. T. Gao, *Appl. Phys. Lett.* **74**, 880 (1999).

⁸M. G. Mason, L. S. Hung, C. W. Tang, S. T. Lee, K. W. Wong, and M. Wang, *J. Appl. Phys.* **86**, 1888 (1999).

⁹Th. Kugler, W. R. Salaneck, H. Rost, and A. B. Holmes, *Chem. Phys. Lett.* **310**, 391 (1999).

¹⁰Q. T. Le, F. Nüesch, L. J. Rothberg, E. W. Forsythe, and Y. Gao, *Appl. Phys. Lett.* **75**, 1357 (1999).

¹¹M. Stössel, J. Staudigel, F. Steuber, J. Simmerer, and A. Winnacker, *Appl. Phys. A: Mater. Sci. Process.* **68**, 387 (1999).

¹²E. I. Haskal, A. Curioni, P. F. Seidler, and W. Andreoni, *Appl. Phys. Lett.* **71**, 1151 (1997).

¹³J. Kido, K. Nagai, and Y. Okamoto, *IEEE Trans. Electron Devices* **40**, 1342 (1993).

¹⁴L. S. Hung, C. W. Tang, and M. G. Mason, *Appl. Phys. Lett.* **70**, 152 (1997).

¹⁵J. Kido and T. Matsumoto, *SID 97 Digest*, 775 (1997).

¹⁶G. E. Jabbour, B. Kippelen, N. R. Armstrong, and N. Peyghambarian, *Appl. Phys. Lett.* **73**, 1185 (1998).

¹⁷P. Raychaudhuri (unpublished, 1999).

¹⁸C. H. Lee, *Synth. Met.* **91**, 125 (1997).

¹⁹T. Wakimoto, Y. Fukuda, K. Nagayama, A. Yokoi, H. Nakada, and M. Tsuchida, *IEEE Trans. Electron Devices* **44**, 1245 (1997).

²⁰G. E. Jabbour, M. M. Morrell, S. E. Shaheen, B. Kippelen, and N. Peyghambarian, 9th International Workshop on Inorganic and Organic Electroluminescence, 1998, p. 49.

²¹L. S. Hung and J. Madathil (unpublished, 1999).

²²See, for example, H. Ishii, K. Kiyoshi, E. Ito, and K. Seki, *Adv. Mater.* **11**, 605 (1999).

²³N. Johansson, T. Osada, S. Stafström, W. R. Salaneck, V. Parente, D. A. dos Santos, X. Crispin, and J. L. Brédas, *J. Chem. Phys.* **111**, 2157 (1999).

²⁴V.-E. Choong, M. G. Mason, C. W. Tang, and Y. Gao, *Appl. Phys. Lett.* **72**, 2689 (1998).

²⁵Q. T. Le, L. Yan, V.-E. Choong, E. W. Forsythe, M. G. Mason, C. W. Tang, and Y. Gao, *Synth. Met.* **102**, 1014 (1999).

²⁶Q. T. Le, M. G. Mason, L. Yan, V.-E. Choong, E. W. Forsythe, C. W. Tang, and Y. Gao, *Proc. SPIE* **3628**, 64 (1999).

²⁷P. E. Burrows, Z. Shen, V. Bulovic, D. M. McCarty, S. R. Forrest, J. A. Cronin, and M. E. Thompson, *J. Appl. Phys.* **79**, 7991 (1996).

²⁸A. Curioni, M. Boero, and W. Andreoni, *Chem. Phys. Lett.* **294**, 263 (1998).

²⁹A. Rajagopal and A. Kahn, *J. Appl. Phys.* **84**, 355 (1998). This cited article did not report the N 1s spectrum. The UPS reported in the cited article is in agreement with ours. All Mg spectra shown in this work were recorded by the authors.

³⁰A. R. Williams, R. A. D. Groot, and C. B. Sommers, *J. Chem. Phys.* **63**, 628 (1975); J. C. Slater, *Adv. Quantum Chem.* **6**, 1 (1972).

³¹A. Curioni, W. Andreoni, R. Treusch, E. Haskal, P. Seidler, C. Heske, S. Kakar, T. van Buuren, and L. J. Terminello, *Appl. Phys. Lett.* **72**, 1575 (1998).

³²M. Probst and R. Haight, *Appl. Phys. Lett.* **70**, 1420 (1997).

³³P. Dannetun, M. Fahlman, C. Fauquet, K. Kaerijama, Y. Sonoda, R. Lazzaroni, J. L. Brédas, and W. R. Salaneck, *Synth. Met.* **67**, 133 (1994).

³⁴C. W. Tang and S. A. VanSlyke, *Appl. Phys. Lett.* **51**, 913 (1987); For this purpose the Mg is typically alloyed with silver to improve the sticking coefficient but the injection properties are thought to be controlled by the low work function Mg.

³⁵S. Naka, M. Tamekawa, T. Terashita, H. Okada, H. Anada, and H. Onnagawa, *Synth. Met.* **91**, 129 (1997).

³⁶K. Seki and H. Ishii, *J. Electron Spectrosc. Relat. Phenom.* **88**, 821 (1998).

³⁷T. Mori, H. Fujikawa, S. Tokito, and Y. Taga, *Appl. Phys. Lett.* **73**, 2763 (1998).

³⁸Q. T. Le, L. Yan, Y. Gao, M. G. Mason, D. J. Giesen, and C. W. Tang, *J. Appl. Phys.* **87**, 375 (2000).

³⁹DFT calculations were run using GAUSSIAN98 rev A.7 with the keywords "B3LYP/3-21G*OPTSCF=(TIGHT,DIRECT)." The energy of the complex is -1904.486 0677 hartree. No exhaustive attempt was made to find lower energy complexes or reaction barriers. The calculation was relatively free of spin contamination with S2=0.759 776 before annihilation and S2A=0.750 074 after. Reference for GAUSSIAN98: M. J. Frisch *et al.*, Gaussian98 Revision A7 Gaussian, Inc, Pittsburgh, PA, 1998.

⁴⁰A. Curioni and W. Andreoni, *J. Am. Chem. Soc.* **121**, 8216 (1999).

⁴¹S. E. Shaheen *et al.*, *J. Appl. Phys.* **84**, 2324 (1998).

⁴²R. Schlaf, B. A. Parkinson, P. A. Lee, K. W. Nebesny, G. Jabbour, B. Kippelen, N. Peyghambarian, and N. R. Armstrong, *J. Appl. Phys.* **84**, 6729 (1998).

⁴³M. Matsumura and Y. Jinde, *Appl. Phys. Lett.* **73**, 2872 (1998).

⁴⁴M. Matsumura, K. Furukawa, and Y. Jinde, *Thin Solid Films* **331**, 96 (1998).

⁴⁵F. Li, H. Tang, J. Anderegg, and J. Shinar, *Appl. Phys. Lett.* **70**, 1233 (1997). In this work a thin Al layer was evaporated onto Alq₃ and then allowed to oxidize. As shown in the present work, Al reacts destructively with Alq₃ so the process used in this reference most certainly did not produce the desired Alq₃/Al₂O₃/Al interface.

- ⁴⁶G. E. Jabbour, Y. Kawabe, S. E. Shaheen, J. F. Wang, M. M. Morrell, B. Kippelen, and N. Peyghambarian, *Appl. Phys. Lett.* **71**, 1762 (1997).
- ⁴⁷Y.-E. Kim, H. Park, and J.-J. Kim, *Appl. Phys. Lett.* **69**, 599 (1996).
- ⁴⁸H. Tang, F. Li, and J. Shinar, *Appl. Phys. Lett.* **71**, 2560 (1997).
- ⁴⁹J. J. Yeh and I. Lindau, *At. Data Nucl. Data Tables* **32**, 1 (1985).
- ⁵⁰T. D. Thomas, *J. Electron Spectrosc. Relat. Phenom.* **20**, 117 (1980).
- ⁵¹When referenced to the vacuum level, the core and valence levels are at constant binding energies with pure metal dopants. This is not true for $\text{Alq}_3/\text{LiF}(\text{CsF})/\text{Al}$ where the binding energy depends on the amount of deposited Al. This is to be expected as the vacuum level will be modified by the presence of metallic Al and its reaction products with Alq_3 and LiF (CsF).
- ⁵²D. D. Wagman, W. H. Evans, V. B. Parker, R. H. Schumm, S. M. Baily, I. Halow, K. L. Churney, and R. L. Nuttall, in *Handbook of Chemistry and Physics*, 67th ed. edited by R. C. Weast, M. J. Astle, and W. H. Beyer (Chemical Rubber Corp., Boca Raton, 1986), p. D-50.
- ⁵³J. A. Kerr, in *Handbook of Chemistry and Physics*, 67th ed., edited by R. C. Weast, M. J. Astle, and W. H. Beyer (Chemical Rubber Corp., Boca Raton, 1986), p. F-167.
- ⁵⁴M. G. Mason, *Phys. Rev. B* **27**, 748 (1983).
- ⁵⁵J. Kido and T. Matsumoto, *Appl. Phys. Lett.* **73**, 2866 (1998).
- ⁵⁶G. Gu, V. Bulovic, P. E. Burrows, S. R. Forrest, and M. E. Thompson, *Appl. Phys. Lett.* **68**, 2606 (1996).
- ⁵⁷V. Bulovic, P. Tian, P. E. Burrows, M. R. Gokhale, S. R. Forrest, and M. E. Thompson, *Appl. Phys. Lett.* **70**, 2954 (1997).
- ⁵⁸G. Parthasarathy, P. E. Burrows, V. Khalfin, V. G. Kozlov, and S. R. Forrest, *Appl. Phys. Lett.* **72**, 2138 (1998).
- ⁵⁹L. S. Hung and C. W. Tang, *Appl. Phys. Lett.* **74**, 3209 (1999).